J|A|C|S ARTICLES

Published on Web 10/09/2009

Theoretical Characterization of the Dynamical Behavior and Transport Properties of α,γ-Peptide Nanotubes in Solution

Rebeca García-Fandiño,[†] Juan R. Granja,[||] Marco D'Abramo,*[,†,‡] and Modesto Orozco[†,‡,§,*]

Institut de Recerca Biomèdica and Instituto Nacional de Bioinformática, Parc Científic de Barcelona, Josep Samitier 1-5, Barcelona 08028, Spain, Computational Biology Program, Barcelona Supercomputer Center, Jordi Girona 31, Edifici Torre Girona, Barcelona 08028, Spain, Departament de Bioquímica, Facultat de Biología, Avgda Diagonal 647, Barcelona 08028, Spain, and Departamento de Química Orgánica, Universidad de Santiago de Compostela, 15782 Santiago de Compostela, Spain

Received April 27, 2009; E-mail: modesto@mmb.pcb.ub.es; marco.dabramo@irbbarcelona.org

Abstract: We present here a molecular dynamics study on a promising class of peptide nanotubes with a partially hydrophobic inner cavity and an easy chemical functionalization of the lumen of the cylindrical structure. The structural and dynamical behavior of the nanotube in water, methanol, and chloroform has been analyzed using state of the art theoretical methods. The nanotube structure is always well preserved, but solvent-dependent dynamic alterations are evident. Such dynamic effects are surprisingly more severe in the most viscous solvent (water), as a consequence of the competition in polar solvents between intra- and intermolecular hydrogen bonds. Stiffness analysis from the collected trajectories helped us to characterize the equilibrium deformability of the nanotube, while steered dynamics simulations were used to determine the magnitude of free energy associated with nanotube growth. Analysis of the carrier and permeation properties of the compounds reveals surprising properties: (i) permeability for the most polar solvent (water), (ii) carrier properties for the most apolar solvent (chloroform), and (iii) neither good permeation nor carrier properties for the intermediate solvent in polarity (methanol). Results reported here constitute the most extensive characterization of these nanotubes presented to date and open many intriguing questions on their stability, dynamics, and transport/carrier properties.

1. Introduction

Self-assembling peptide nanotubes (SPNs) have attracted a great amount of attention from the scientific community in recent years due to their important applications in biology, chemistry and material science.[1] A large part of this interest is related to their technological possibilities as biosensors, photosensitive materials, antimicrobial agents, selective transporter systems, molecular electronics components, and other potential uses in biology, electronics, and optics.[2] The history of nanotubes started in 1974, when De Santis[3] predicted the formation of tubular structures by cyclic peptides, formed by α-amino acids of alternant D and L stereochemistry. However, the first peptide nanotubes were not prepared until 1993 by Ghadiri et al.[4] Other types of peptide nanotubes have been created since then using

[†] IRBB Parc Cientific de Barcelona.
[‡] Barcelona Supercomputer Centre.
[§] Departament de Bioquímica. Universitat de Barcelona.
[||] Departamento de Química Orgánica. Universidad de Santiago de Compostela.

(1) (a) Hartgerink, J. D.; Clark, T. D.; Ghadiri, M. R. *Chem.—Eur. J.* **1998**, *4*, 1367. (b) Brea, R. J.; Granja, J. R. *Dekker Encyclopedia of Nanoscience and Nanotechnology*; Marcel Dekker Inc.: 2004; Monticello, NY; p 3439. (c) Patzke, G. R.; Krumeich, F.; Nesper, R. *Angew. Chem., Int. Ed.* **2002**, *41*, 2446; *Angew. Chem.* **2002**, *114*, 2554. (d) Bong, D. T.; Clark, T. D.; Granja, J. R.; Ghadiri, M. R. *Angew. Chem., Int. Ed.* **2001**, *40*, 988; *Angew. Chem.* **2001**, *113*, 1016. (e) Ajayan, P. M.; Zhou, O. Z. *Top. Appl. Phys.* **2001**, *80*, 391. (f) Janshoff, A.; Dancil, K. P. S.; Steinem, C.; Greiner, D.; Lin, P. V. S. Y.; Gurtner, C.; Motesharei, K.; Sailor, M. J.; Ghadiri, M. R. *J. Am. Chem. Soc.* **1998**, *120*, 12108. (g) David, G.; Pierre, B. M. *Angew. Chem., Int. Ed.* **2001**, *40*, 4635. (h) Ghadiri, M. R. *Adv. Mater.* **1995**, 675.

(2) For some of the most important applications of peptide nanotubes, see for example: (a) Ghadiri, M. R.; Granja, J. R.; Buehler, L. K. *Nature* **1994**, *369*, 301. (b) Granja, J. R.; Ghadiri, M. R. *J. Am. Chem. Soc.* **1994**, *116*, 10785. (c) Sanchez-Quesada, J.; Kim, H. S.; Ghadiri, M. R. *Angew. Chem., Int. Ed.* **2001**, *40*, 2503. (d) Fernandez-Lopez, S.; Kim, H. S.; Choi, E. C.; Delgado, M.; Granja, J. R.; Khasanov, A.; Kraehenbuehl, K.; Long, G.; Weinberger, D. A.; Wilcoxen, K. M.; Ghadiri, M. R. *Nature* **2001**, *412*, 452. (e) Sanchez-Quesada, J.; Ghadiri, M. R.; Bayley, H.; Braha, O. *J. Am. Chem. Soc.* **2000**, *122*, 11757. (f) Clark, T. D.; Buehler, L. K.; Ghadiri, M. R. *J. Am. Chem. Soc.* **1998**, *120*, 651. (g) Horne, W. S.; Ashkenasy, N.; Ghadiri, M. R. *Chem.—Eur. J.* **2005**, *11*, 1137. (h) Ortiz-Acevedo, A.; Xie, H.; Zorbas, V.; Sampson, W. M.; Dalton, A. B.; Baughman, R. H.; Draper, R. K.; Musselman, I. H.; Dieckmann, G. R. *J. Am. Chem. Soc.* **2005**, *127*, 9512. (i) Martin, C. R.; Kohli, P. *Nat. Rev. Drug Discovery* **2003**, *2*, 29. (j) Gao, X.; Matsui, H. *Adv. Mater.* **2005**, *17*, 2037. (k) Dartois, V.; Sanchez-Quesada, J.; Cabezas, E.; Chi, E.; Dubbelde, C.; Dunn, C.; Gritzen, C.; Weinberger, D.; Granja, J. R.; Ghadiri, M. R.; Parr, T. R., Jr. *Antimicrob. Agents Chemother.* **2005**, *49*, 3302. (l) Steinem, C.; Janshoff, A.; Vollmer, M. S.; Ghadiri, M. R. *Langmuir* **1999**, *15*, 3956. (m) Vollmer, M. S.; Clark, T. D.; Steinem, C.; Ghadiri, M. R. *Angew. Chem., Int. Ed.* **1999**, *38*, 1598. (n) Motesharei, K.; Ghadiri, M. R. *J. Am. Chem. Soc.* **1997**, *119*, 11306. (o) Couet, J.; Samuel, J. D. J. S.; Kopyshev, A.; Santer, S.; Biesalski, M. *Angew. Chem., Int. Ed.* **2005**, *44*, 3297. (p) Ashkenasy, N.; Horne, W. S.; Ghadiri, M. R. *Small* **2006**, *2*, 99.

(3) De Santis, P.; Morosetti, S.; Rizzo, R. *Macromolecules* **1974**, *7*, 52.

(4) Ghadiri, M. R.; Granja, J. R.; Milligan, R. A.; McRee, D. E.; Khazanovich, N. *Nature* **1993**, *366*, 324.

10.1021/ja903400n CCC: $40.75

Scheme 1. Representation of Self-Assembling Peptide Nanotubes Composed of *cyclo*-[(1*R*,3*S*)-γ-Ach-*D*-Aa]$_3$ Units[a]

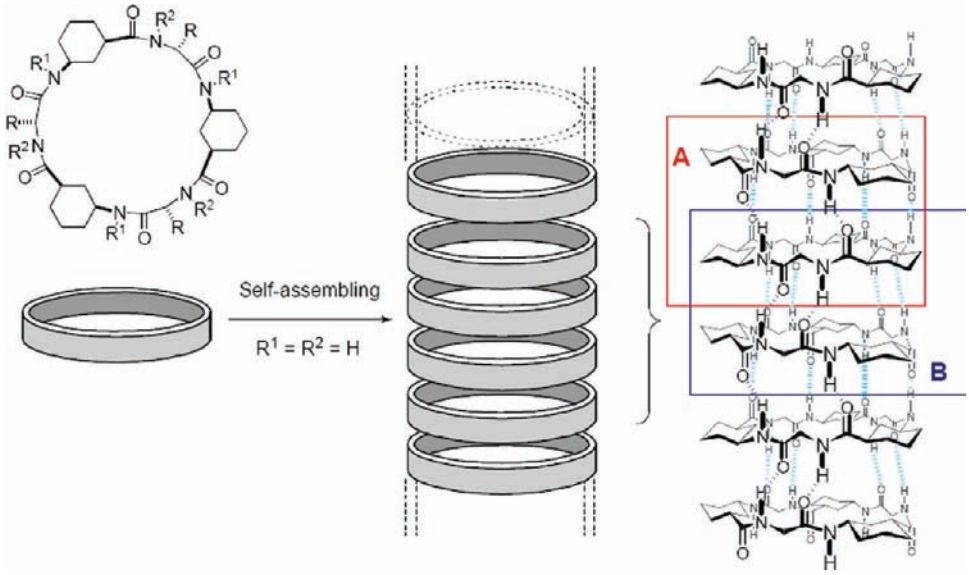

[a] For clarity, amino acid side chains have been omitted. The two different H-bonding patterns (A for γ−γ and B for α−α) are shown in different colors.

different amino acids,[2f,5] including those consisting of alternating (1*R*,3*S*)-3-aminocycloalkanecarboxyl acid (Aca) and D-α-amino acid (α, γ-SPN).[6] In all of them, the chiralities of the amino acids allow the ring to adopt a quasi-planar conformation, where the peptide backbone N−H and C═O groups lay perpendicular to the ring plane on either side and are therefore able to form hydrogen bonds with those of neighboring rings, thus leading to the formation of tubular nanotube structures (Scheme 1). The α,γ-SPN involves two different sets of β-sheet-like hydrogen bonds: one exclusively involves the NH and C═O groups of the γ-amino acids (γ−γ, A in Scheme 1), and the other, apparently slightly more stable,[6a,b] engages the same groups of the α-amino acids (α−α bonding, B in Scheme 1).

While almost all the cyclic peptide nanotubes that have been developed so far have hydrophilic inner surfaces and can only permeate polar molecules, in the case of the α,γ-SPN, the C2 methylene group of each cycloalkane moiety is projected into the lumen of the cylinder, generating a partially hydrophobic cavity, which can be modulated by simple chemical modification of the β-carbon of the cyclic γ-Acas, allowing, in principle, finer control of the transport properties of the nanotube.

Despite the increasing knowledge on peptide nanotubes, there are many aspects of their microscopic behavior that remain obscure, like their structural variability with solvent, dynamics, deformability, energetic landscapes, the nature of the intra- and intermolecular interactions stabilizing the nanotube, and their properties as a molecular transporter (i.e., as a molecule able to permeate the ligand from one side to the other of the nanotube) or container (i.e., to store the ligand). Theoretical calculations would largely improve our knowledge on all these details, but in contrast to the large amount of theoretical work on "classical" D,L-α-SPN,[7] very little theoretical work has been done on α,γ-SPN.[8] In this paper we present for the first time a complete theoretical analysis of a peptide nanotube consisting of alternating (1*R*,3*S*)-3-aminocyclohexanecarboxyl acid and D-α-amino acid formed by six cyclopeptide (CP) units, analogous to the system experimentally investigated.[6a] The results obtained allow the full characterization of the structural, energetic, dynamic, and transport properties of this interesting new class of nanotubes and suggest interesting possibilities for the design of new nanotube derivatives.

2. Materials and Methods

The nanotube atomic coordinates were obtained from a previous X-ray crystal structure with dimer-forming methyl-blocked CP *cyclo*-[(D-Phe-(1*R*,3*S*)-^{Me}N-γ-Ach)$_3$-].[6a] The resolved cylindrical dimer has an approximate van der Waals internal diameter of 5.4 Å and a volume of 165 Å^3. From this structure, the N-groups were removed and the side chains of the α-amino acid were substituted

(5) (a) Seebach, D.; Matthews, J. L.; Meden, A.; Wessels, T.; Baerlocher, C.; McCusker, L. B. *Helv. Chim. Acta* **1997**, *80*, 173. (b) Karle, I. L.; Handa, B. K.; Hassall, C. H. *Acta Crystallogr., Sect. B* **1975**, *31*, 555. (c) Gauthier, D.; Baillargeon, P; Drouin, M; Dory, Y. L. *Angew. Chem., Int. Ed.* **2001**, *40*, 4635; *Angew. Chem.* **2001**, *113*, 4771. (d) Leclair, S.; Baillargeon, P.; Skouta, R.; Gauthier, D.; Zhao, Y.; Dory, Y. L. *Angew. Chem., Int. Ed.* **2004**, *43*, 349; *Angew. Chem.* **2004**, *116*, 353. (e) Horne, W. S.; Stout, C. D.; Ghadiri, M. R. *J. Am. Chem. Soc.* **2003**, *125*, 9372. (f) Ranganathan, D.; Lakshmi, C.; Karle, I. L. *J. Am. Chem. Soc.* **1999**, *121*, 6103. (g) Semetey, V.; Didierjean, C.; Briand, J. P.; Aubry, A.; G. Guichard, G. *Angew. Chem., Int. Ed.* **2002**, *41*, 1895; *Angew. Chem.* **2002**, *114*, 1975. (h) Shimizu, L. S.; Hughes, A. D.; Smith, M. D.; Davis, M. J.; Zhang, B. P.; Loye, H.-C; Shimizu, K. D. *J. Am. Chem. Soc.* **2003**, *125*, 14972.

(6) (a) Amorín, M.; Castedo, L.; Granja, J. R. *J. Am. Chem. Soc.* **2003**, *125*, 2844. (b) Amorín, M.; Castedo, L.; Granja, J. R. *Chem.—Eur. J.* **2005**, *11*, 6543. (c) Brea, R. J.; Amorín, M.; Castedo, L.; Granja, J. R. *Angew. Chem., Int. Ed.* **2005**, *44*, 5710. (d) Amorín, M.; Brea, R. J.; Castedo, L.; Granja, J. R. *Org. Lett.* **2005**, *7*, 4681. (e) Brea, R. J.; Castedo, L.; Granja, J. R. *Chem. Commun.* **2007**, *31*, 3267. (f) Amorín, M.; Castedo, L.; Granja, J. R. *Chem.—Eur. J.* **2008**, *14*, 2100. (g) Brea, R. J.; Vázquez, R. M. E.; Mosquera, M.; Castedo, L.; Granja, J. R. *J. Am. Chem. Soc.* **2007**, *129*, 1653. (h) Brea, R. J.; Castedo, L.; Granja, J. R.; Herranz, M. A.; Sánchez, L.; Martín, N.; Seitz, W.; Guldi, D. M. *Proc. Natl. Acad. Sci. U.S.A.* **2007**, *104*, 5291. (i) Amorín, M.; Villaverde, V.; Castedo, L.; Granja, J. R. *J. Drug Delivery Sci. Technol.* **2005**, *15*, 87.

(7) (a) Engels, M.; Bashford, D.; Ghadiri, M. R. *J. Am. Chem. Soc.* **1995**, *117*, 9151. (b) Lewis, J. P.; Pawley, N. H.; Sankey, O. F. *J. Phys. Chem. B* **1997**, *101*, 10576. (c) Jishi, R. A.; Flores, R. M.; Valderrama, M.; Lou, L.; Bragin, J. *J. Phys. Chem. A* **1998**, *102*, 9858. (d) Chen, G.; Su, S.; Liu, R. *J. Phys. Chem. B* **2002**, *106*, 1570. (e) Tarek, M.; Maigret, B.; Chipot, C. *Biophys. J.* **2003**, *85*, 2287. (f) Hwang, H.; Schatz, G. C.; Ratner, M. A. *J. Phys. Chem. B* **2006**, *110*, 26448. (g) Hwang, H.; Schatz, G. C.; Ratner, M. A. *J. Phys. Chem. B* **2006**, *110*, 6999. (h) Chipot, C.; Tarek, M. *Phys. Biol.* **2006**, *3*, S20.

(8) Cheng, J.; Zhu, J.; Liu, B. *Chem. Phys.* **2007**, *333*, 105.

by methyl groups, since it has been proven that they do not have any significant effect over the global stability of the nanotube.[6b] This dimer was then replicated twice along the axis perpendicular to the cyclic peptide planes, by a distance equal to that measured between the two original CP units. Therefore, the resulting nanotube is composed by six cyclopeptide units. Starting from this structure, molecular dynamics simulations (MD) of a single SPN were performed at 300 K in water, chloroform, and methanol at their respective experimental densities using the Gromacs software package.[9] Unless otherwise noted, during the solvation step, the solvent molecules present in the SPN inner cavity were removed. The water was simulated using the SPC model,[10] methanol parameters for most calculations were taken from the work of van Gunsteren and co-workers,[11a] but additional tests were performed with Jorgensen's OPLS all atoms force-field[11b] finding no significant difference with the van Gunsteren united atom model (see Supporting Information, Figure S7); the chloroform model is taken from AMBER parameters.[12] Concerning the atoms of the SPN, RESP/6-31G(d) charges were derived as in the original AMBER force-field development, while van der Waals parameters were taken from the GAFF software[13] using standard Lorenz−Bertelot combination rules. Bonded terms were taken as those of standard peptides.

All the systems were partially optimized, thermalized, and equilibrated using our standard protocol,[14] followed by unrestrained simulations for at least 20 ns (time step = 2 fs) at constant volume and temperature using the Berendsen thermal coupling, and the energies and coordinates were recorded every 2 ps. Due to the slow kinetics, simulations in chloroform and in methanol were extended to 300 and 200 ns, respectively. The LINCS[15] algorithm was employed to remove the bond vibrations. The Particle Mesh Ewald method[16] coupled to periodic boundary conditions was used to treat the long-range electrostatics using a direct-space cutoff of 1.0 nm and a grid spacing of 0.12 nm. van der Waals interactions were computed using PBC coupled to a spherical cutoff of 1.0 nm.

To check whether simulations with apolar solvents were contaminated from memory artifacts, we performed additional simulations for chloroform and methanol starting from configurations where the channel of the NT was manually filled with solvent molecules. These systems were partially optimized, thermalized and equilibrated (using the same protocol noted above), and subjected to 0.1 μs of unrestrained MD simulation. Finally, to check whether the low diffusion of chloroform inside the channel was not a simulation artifact, we selected 100 independent structures from the first 10 ns of the (0.3 μs) chloroform trajectory, adding random velocities to all atoms (taken care of maintaining the same temperature) and using the resulting files to perform 100 independent 1 ns simulations.

To count the number of solvent molecules filling the SPN internal cavity, the equation of a cylinder with the major axis passing through the center of mass and the radius equal to the radius of the rings was solved for every MD frame (see Scheme 1) and used to define the NT boundaries. The flexibility of the NT was analyzed in terms of rotations and translations between stacked CPs, showing an almost complete rigidity except for the translation along the major axis. Such a degree of freedom produces a deformability on the structure that, assuming harmonic behavior, can be described by eq 1,

$$E = K/2(X - X_o)^2 \quad (1)$$

where X and X_o stand for the actual and equilibrium inter-ring distance, and the stiffness constant (K) is derived from the inter-ring distance fluctuations (ΔX^2; see eq 2)

$$K = k_B T/\langle \Delta X^2 \rangle \quad (2)$$

where k_B is the Boltzmann constant and T is the absolute temperature (300 K in our case).

We completed our set of analysis performing steered MD simulations (in chloroform, in water, and in methanol) based on Jarzynski's equality and the stiff-spring approximation to estimate the free energy needed to pull away one (terminal) cyclopeptide unit (ΔA_{TOT}). The center of mass (c.o.m.) coordinates of the first five rings were kept fixed, and the sixth ring was pulled away (along the SPN major axis) with speeds and force constants ranging from 0.00025 to 0.001 nm ps^{-1} and from 10000 to 25000 kJ mol^{-1} nm^{-2}, respectively (such a range of conditions helped to gain confidence in the final estimates). To remove errors arising from the use of excessively large pulling velocities, additional steered MD simulations of a single cyclopeptide unit (in solvent) were performed using the same conditions as those in the pulling simulations in the presence of the nanotube. The computed work (which in ideal conditions should be nil) was subtracted from ΔA_{TOT} to obtain an unbiased estimate of the potential of mean force. The second order cumulant approximation as well as the full exponential formula was applied to obtain the free energy values. Every free energy estimate was obtained by performing 100 pulling runs starting from different and uncorrelated configurations. The speed was lowered to a quarter of the original one in the regions where the sampling was originally poor. Such a conservative and very CPU-consuming protocol is expected to provide accurate estimates in our system.[23]

The self-diffusion coefficients for the solvent molecules were computed using the Einstein relation [eq 3]:

$$\lim_{t\to\infty} \langle ||r_i(t) - r_i(0)||^2 \rangle_{ieA} = 2gD_A t \quad (3)$$

where g is the number of degrees of freedom, D_A is the diffusion constant for molecule A, and $r_i(t)$ is the position vector at time t. Although the trajectories (20 ns) could not be long enough to accurately determine the transport properties all along the SPN, an estimate of the ratio of the self-diffusion coefficient between the solvent molecules inside and outside the SPN was used to provide

(9) Lindahl, E.; Hess, B.; van der Spoel, D. J. *Mol. Mod.* **2001**, *7*, 306.
(10) Berendsen, H. J. C.; Postma, J. P. M.; van Gunsteren, W. F.; Hermans, J. In *Intermolecular Forces*; Pullman, B., Ed.; Reidel: Dordrecht, 1981; p 331.
(11) (a) Walser, R.; Mark, A. E.; van Gunsteren, W. F.; Lauterbach, M.; Wipff, G. *J. Chem. Phys.* **2000**, *112*, 10450. (b) Jorgensen, W. L.; Maxwell, D. S.; Tirado-Rives, J. *J. Am. Chem. Soc.* **1996**, *118*, 11225.
(12) (a) Fox, T.; Kollman, P. *J. Phys. Chem. B* **1998**, *102*, 8070. (b) Cieplak, P.; Caldwell, J.; Kollman, P. *J. Comput. Chem.* **2001**, *22*, 1048.
(13) (a) Wang, J.; Wang, W.; Kollman, P. A.; Case, D. A. *J. Mol. Graphics Modell.* **2006**, *25*, 247260. (b) Wang, J.; Wolf, R. M.; Caldwell, J. W.; Kollman, P. A.; Case, D. A. *J. Comput. Chem.* **2004**, *25*, 1157.
(14) Shields, G. C.; Laughton, C. A.; Orozco, M. *J. Am. Chem. Soc.* **1997**, *119*, 7463.
(15) Hess, B.; Bekker, H.; Berendsen, H. J. C.; Fraaije, J. G. E. M. *J. Comput. Chem.* **1997**, *18*, 1463.
(16) Essman, U.; Perera, L.; Berkowitz, M.; Darden, T.; Lee, H.; Pedersen, L. *J. Chem. Phys.* **1995**, *103*, 8577.
(17) Gelpi, J. L.; Kalko, S. G.; Barril, X.; Cirera, J.; de la Cruz, X.; Luque, F. J.; Orozco, M. *Proteins* **2001**, *45*, 428.
(18) We consider that a hydrogen bond exists if the distance between the donor and acceptor atoms is less than 0.35 nm and the A−D−H angle is less than 30°, where A, D, and H represent the acceptor, donor, and hydrogen atom, respectively.
(19) Clark, T. D.; Buriak, J. M.; Kobayashi, K.; Isler, M. P.; McRee, D. E.; Ghadiri, M. R. *J. Am. Chem. Soc.* **1998**, *120*, 8949.
(20) Perez, A.; Lankas, F.; Luque, F. J.; Orozco, M. *Nucleic Acids Res.* **2008**, *36*, 2379.
(21) Rueda, M.; Ferrer-Costa, C.; Meyer, T.; Pérez, A.; Camps, J.; Hospital, A.; Gelpí, J. L.; Orozco, M. *Proc. Natl. Acad. Sci. U.S.A.* **2007**, *104*, 796.
(22) (a) Crooks, G. E. *Phys. Rev. E* **1999**, *60*, 2721. (b) Collin, D.; Ritort, F.; Jarzynski, C.; Smith, S. B.; Tinoco, I., Jr.; Bustamante, C. *Nature* **2005**, *437*, 231.
(23) (a) Jarzynski, C. *Phys. Rev. Lett.* **1997**, *78*, 2690. (b) Jensen, M. O.; Park, S.; Tajkhorshid, E.; Schulten, K. *Proc. Natl. Acad. Sci. U.S.A.* **2002**, *99*, 6731. (c) Amaro, R.; Tajkhorshid, E.; Schulten, Z. L. *Proc. Natl. Acad. Sci. U.S.A.* **2003**, *100*, 7599.

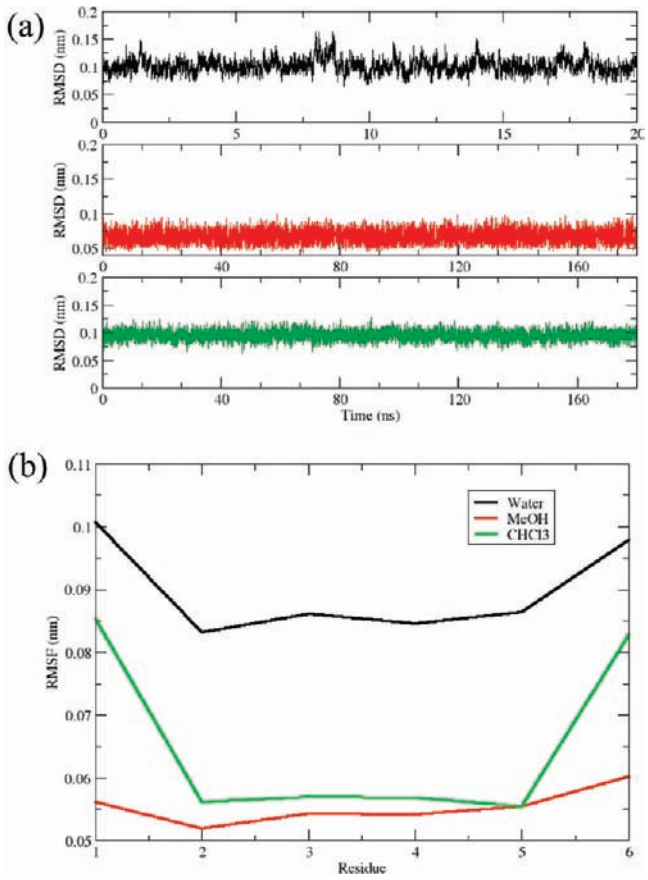

Figure 1. (a) RMSd of the peptide nanotube in water (black), methanol (red), and chloroform (green). (b) RMSf per cyclopeptide unit for the nanotube in water (black), methanol (red), and chloroform (green).

further information on the corresponding diffusional behavior. Molecular interaction potential calculations to explore the internal cavity of the nanotube were performed with the Classical Molecular Interaction Potential (cMIP) program.[17] For this purpose, the interaction energies between a neutral carbon probe placed in a 0.5 Å spacing grid covering the overall structure were measured. The total interaction energy was determined as the sum of electrostatic and van der Waals interactions (the latter considering a neutral second row element).

3. Results and Discussion

The nanotube created by addition of CPs is a very stable and quite rigid entity, as noted in the value of the root-mean-square deviations (RMSd) between the sampled structures and the reference X-ray conformation (see Figure 1a). Analysis of the radii of gyration and of the Ramachandran maps (see Supporting Information) confirms the lack of any major global or local structural distortion during the trajectories and the pure β-sheet-like nature of the cyclopeptides. The solvent has a moderated, but not negligible, influence on the structure of the molecules, as seen in the RMSd plot (Figure 1a), and a major influence on the flexibility, as noted in the root-mean-square fluctuations (RMSf) per cyclopeptide (Figure 1b), which illustrates that the structure is more flexible in water than in the other two solvents. The RMSf plots also show the difference between central (more rigid) and terminal parts (more flexible), a factor that is especially clear in the chloroform simulations (see below).

Analysis of the intramolecular hydrogen bond (H-bond) scheme in water reveals many interesting features: there is an average loss of 0.5−1 intramolecular hydrogen bonds per CP

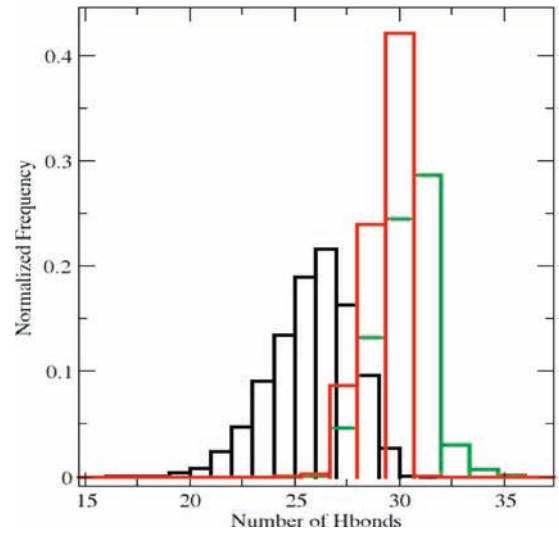

Figure 2. Normalized distribution of the number of hydrogen bonds between (a) nanotube−nanotube in water (black), methanol (red), and chloroform (green).

Table 1. Mean and Standard Deviation of the Number of Hydrogen Bonds between the Cyclic Peptides in Water, Methanol, and Chloroform[a]

	Water		Methanol		Chloroform	
Cyclopeptide / interaction	Mean	Stdev	Mean	Stdev	Mean	Stdev
1-2 (α-α)	5.4	0.8	5.9	0.4	5.2	0.9
2-3 (γ-γ)	5.0	1.0	5.9	0.3	6.0	0.2
3-4 (α-α)	5.6	0.6	5.9	0.3	6.0	0.2
4-5 (γ-γ)	5.0	1.0	5.9	0.3	6.0	0.2
5-6 (α-α)	5.4	0.8	5.8	0.5	5.2	0.8

[a] The order of the cyclic peptides is indicated in the picture on the side.

Table 2. Peptide−peptide H-Bond Energies (in kJ/mol) Calculated by the Interaction between the Six Acceptor−Donor Pairs Present in Cyclopeptide Rings 2 and 3 (for $\gamma-\gamma$ Interaction) or Rings 3 and 4 (for α−α Interaction)[a]

	water		methanol		chloroform	
cyclopeptide/interaction	mean	Stdev	mean	Stdev	mean	Stdev
2−3 (γ−γ)	−10.8	0.3	−12.9	0.2	−13.1	0.2
3−4 (α−α)	−12.2	0.1	−13.6	0.3	−13.9	0.1

[a] Mean and Stdev values correspond to the six H-bonds studied. The order of the cyclic peptides is indicated in Table 1.

(Figure 2 and Table 1) with respect to the theoretical maximum (30)[18] (due to the competition with water molecules; see below), which also explains the larger flexibility of the SPN in water compared to other solvents. It is worth noting that the most labile H-bonds are those involving the γ-Acc C═O and N−H groups ($\gamma-\gamma$ H-bonds), which is a consequence of their intrinsic lower interaction energy (see Table 2). These findings are in agreement with experimental evidence supporting that, despite the similarity in interacting groups, $\gamma-\gamma$ H-bonds are weaker than those involving the C═O and N−H groups of the α-amino acids (α−α H-bonds).[6a,b] The more suitable H-bond geometry in the last case seems to be the major factor responsible for the surprising difference in stability between both types of H-bonds.

In methanol (Figure 2 and Table 1) the number of intramolecular hydrogen bonds is close to the theoretical maximum, while in the most apolar solvent (chloroform) the number of intramolecular H-bonds formed is superior to the theoretical maximum (Figure 2), due mainly to the formation of intraring H-bonds between the free C═O and N−H of γ-amino acids situated at the terminal monomers. The fast interchange between normal inter-rings and unusual intra-ring H-bonds between the free γ-amino acids situated in the solvent exposed γ-face of the SPN is responsible for the anomalously large flexibility on terminal CPs in the chloroform simulations. Control MD simulations of the analogous nanotube with alternated $\alpha-\alpha$/$\gamma-\gamma$ interactions confirm the source of these unexpected additional hydrogen bonds in chloroform and its connection with a higher flexibility at the ends of the nanotube (see Supporting Information). Energy analysis for central peptides (Table 2) confirms that the weakest H-bonds are found in water and the strongest ones in chloroform and methanol.

Both water and methanol have hydrogen-bond capabilities, and accordingly, SPN intramolecular H-bonds have to compete with CP−water interactions. This is clearly shown in Figure 3a and 3b, which illustrate how the higher propensity of water to form H-bonds overcompensates for the loss of intramolecular SPN contacts. The situation in methanol is different, since, on average, only 10 hydrogen bonds are formed between the cyclopeptides and the solvent, and there is just a residual correlation between the loss of intramolecular and intermolecular H-bonds. Energy calculations in Table 2 confirm that methanol has an almost negligible (closer to that of chloroform) ability to interfere in peptide−peptide H-bonding interactions. All together this means that water is able to compete with CP−CP interactions hindering the assembly of the nanotube, while methanol (and obviously chloroform) cannot (see below, Table 1). As a result, methanol is then less impactful in disturbing the stability of the structure than water, as suggested by Ghadiri and co-workers in D,L-α-SPN.[19]

A useful approach to understand nanotube deformability is to assume that it is formed by a stack of cyclic hexapeptides, which can displace one with respect to the other by three 120° rotations and three translations. Analysis of trajectories reveals almost complete rigidity in terms of rotations and translations except for translation along the major axis of the nanotube. Assuming a harmonic behavior (a quite reasonable approximation in this case) the translational deformability along the major axis can be described by the associated stiffness constant (see eqs 1 and 2 in Materials and Methods). Values obtained (considering only the internal units) from the analysis of inter-ring distances obtained from the trajectories range between 29000 kJ mol^{-1} nm^{-2} (water) and 80000 kJ mol^{-1} nm^{-2} (chloroform), which for water represents values approximately 9 times larger than those of a B-DNA duplex,[20] confirming the high rigidity of the nanotube already evident in RMSd and RMSf plots. Clearly, the large amount of stiffness of the nanotube is guided by the strength of the inter-ring hydrogen bonds, as noted in the fact that the force constant per amino acid pair of the nanotube in chloroform (13000 kJ mol^{-1} nm^{-2}) matches the force constant estimated for internal H-bonds in proteins.[21]

To complete the deformability analysis we considered non-harmonic deformations like those needed for the assembly/disassembly of the nanotube. For this purpose, we performed biased simulations, where one of the CPs was forced to leave the nanotube. Using Crooks theorem[22] and the Jarzynski inequality[23] (see Materials and Methods), we computed the potential of mean force (PMF) associated with the detachment of a cyclic peptide from the SPN in the three solvents. PMFs reveal a free energy difference between 57 and 61 kJ mol^{-1} (depending on pulling conditions used in the steered MD simulation) between the unbound and bound form in chloroform (a value that agrees qualitatively well with the experimental estimate obtained for the capped dimer: $\Delta G \geq 34.5$ kJ mol^{-1}[16a]), 58 and 61 kJ mol^{-1} in methanol and 25 and 28 kJ mol^{-1} in water (no experimental data exist in these other two solvents). Standard deviations in each individual estimate (obtained by averaging 100 independent trajectories) were in the range 6−10 kJ mol^{-1}. Further information on the reliability of these results is provided as Supporting Information, Table S1 and Figure S8. Clearly, Steered Molecular Dynamics shows the high stability of the CPs in both very polar and very apolar solvents which reinforces the possibility of these SPNs to exist in a mixed environment like biological membranes, increasing the interest in analyzing these molecules as potential biological channels. In any case, it is clear that the present cyclopeptidic nanotubes

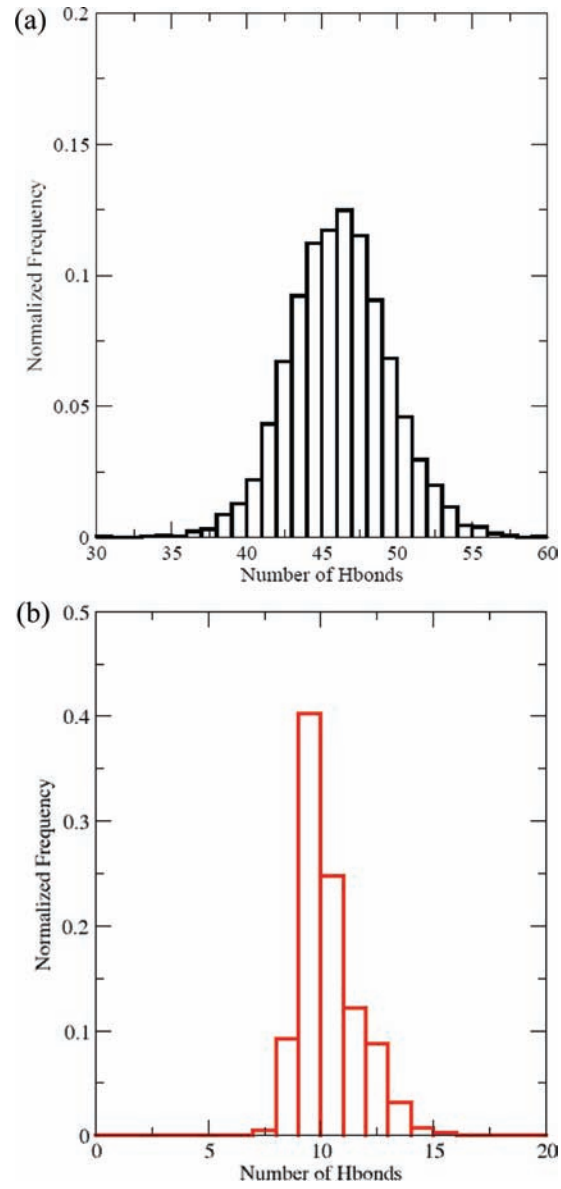

Figure 3. Normalized distribution of the number of hydrogen bonds between (a) nanotube−water and (b) nanotube−methanol.

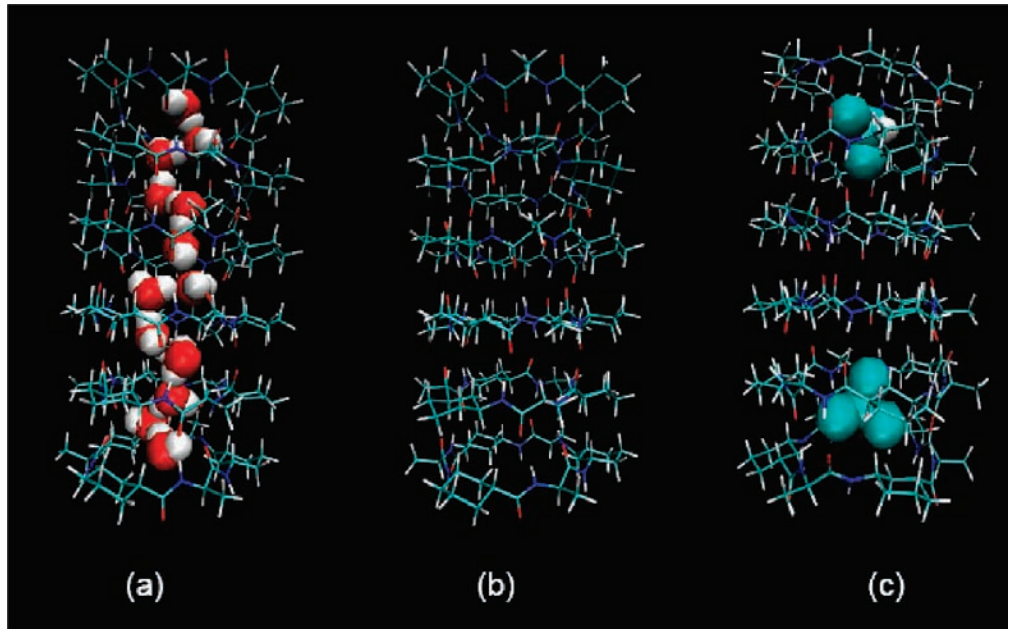

Figure 4. Last snapshots of the trajectory after 20 ns of simulation of the nanotube in (a) water, (b) methanol, and (c) chloroform.

are higher in stability compared with the octameric D,L-α-SPN prepared by Ghadiri and co-workers,[24] for which an association free energy of 29.3 ± 4.2 kJ mol^{-1} was estimated using a similar computational methodology.[25]

A very interesting aspect of SPNs is their ability to act as selective transporters (channels) or containers for small molecules (see Introduction). Unfortunately, the transport properties of the SPNs against different molecules are difficult to predict by simple structure inspection, and the experimental study of these transport properties is complex and tedious. It is then another area where simulations can offer an interesting alternative. To this end, we analyzed the dynamics of solvent molecules inside the nanotube central cavity (see Materials and Methods). Analysis of trajectories reveals a tremendous difference in the transport properties of the SPN for the three solvents considered. Thus, methanol molecules, with relaxation times in the picosecond time scale, refuse to enter spontaneously during multinanosecond long trajectories (see Figure 4), suggesting that the present SPN is not a good transporter and probably not a good carrier for methanol due to the very low kinetic entry constant k^{on}. An additional 100 ns simulation starting with the channel filled manually with methanol molecules showed that the state represented by filled solvent SPN is quite unstable, as demonstrated by the very fast and irreversible exit of the inner solvent molecules (see Supporting Information, Figure S6). The situation in chloroform is clearly different, since diffusion inside the cavity is slow (multinanosecond scale), probably because of the polar nature of the external border of the nanotube, but once inside the nanotube chloroform molecules are stable for the remaining length (300 ns) of the simulation (Figure S5). However, neither 20 nor 300 ns simulations are able to detect the transport of chloroform across the internal pore, suggesting that the hydrophobic environment of the α,γ-SPN interior can act as a good container for nonpolar molecules such as chloroform, but in the absence of external forces it does not seem to be a good transporter. To verify that the NT can be a good container for chloroform despite the bad entry kinetics, we performed one 100 ns simulation manually filling the channel with chloroform molecules. The filled configuration was stable for the entire simulation and undistinguishable from that obtained from 300 ns simulations (Figure S5). Finally, to gain extra confidence on the slow kinetics of solvent diffusion inside the channel, we performed (see Materials and Methods) 100 additional MD simulations of 1 ns, showing that in only 4 of the 100 trajectories the solvent molecules appear in the inner of the SPN cavity at the end of the simulation. Such results explain surprising experimental data on the capped dimers: crystallizations made in chloroform by vapor-phase equilibration with hexane detected one chloroform molecule inside its internal cavity, while analogous experiments using a mixture of methanol/hexane did not show any methanol inside. Instead, water molecules coming from humidity appeared in its inner lumen in crystal structures.[6i]

A completely different scenario is found for water, where despite the expected hydrophobicity of the interior of the channel, we observed significant amounts of water in more than 80% of configurations, with typically ∼13−16 water molecules being placed inside the channel (Figures 4 and 5). This spine of hydration is formed already in the equilibration portion of the trajectory (less than 600 ps), confirming the ability of the nanotube to capture water (already suggested by crystallization experiments; see above). Analysis of solvent densities in the channel allowed us to determine the free energy associated with transfer of a water molecule across the internal cavity of the nanotube. As noted in Figure 6, a flat free energy profile is found and only 4 kJ mol^{-1} are required to reach the center of the channel. Water molecules inside the cavity are placed between the CP planes (Figure 7a) to minimize steric repulsions and to establish H-bonding interactions with the nanotube H-bond donor/

(24) Ghadiri, R. M.; Kobayashi, K.; Granja, J. R.; Chadha, R. K.; McRee, D. E. *Angew. Chem., Int. Ed. Engl.* **1995**, *34*, 95.

(25) Khurana, E.; Nielsen, S. O.; Ensing, B.; Klein, M. L. *J. Phys. Chem. B* **2006**, *110*, 18965. It is worth to mentioning that the theoretical estimate of the free energy, which corresponds to a value of $K_a = 1.2 \times 10^5$ M^{-1}, refers to the *cyclo*-[(-L-Trp-D-MeN-Leu-)$_4$-]$_2$ in nonane whereas the K_a experimentally determined in ref 24 was obtained for CPs made up of different amino acid residues in a different solvent ($CDCl_3$).

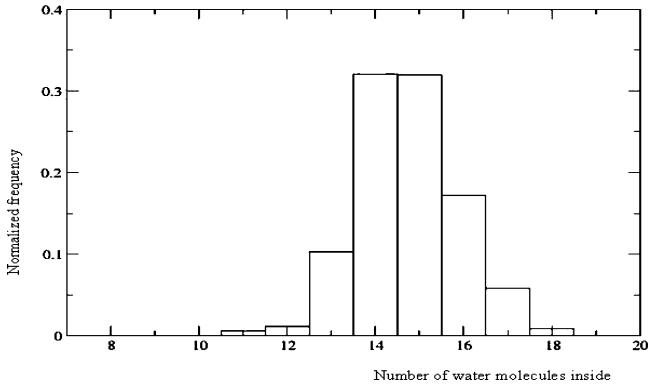

Figure 5. Distribution of the number of water molecules filling the nanotube.

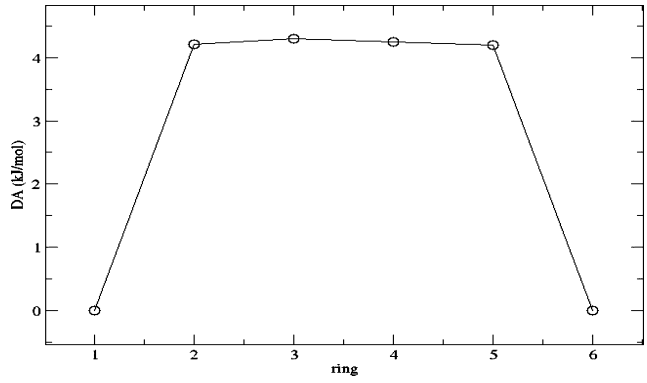

Figure 6. Water free energy profile along the axial axis of the nanotube.

acceptor groups (especially for the γ-ones). CMIP contours in Figure 7b illustrate very well the discontinuity[7a] of the hydration spine in the nanotube. A detailed investigation on the water density also shows that the fluctuations in the number of solvent molecules present between the rings forming $\gamma-\gamma$-interactions, e.g. rings 2−3 and 4−5, are more pronounced than those found between the $\alpha-\alpha$-interactions (see Supporting Information, Figure S4). This agrees with the lower degree of conservation observed for the $\gamma-\gamma$ H-bonding interactions (Table 1), and with the larger effective pore radius found for these regions, calculated by using the HOLE software package (Figure 8).[26]

The ability of the interior of the SPN to dynamically form transient H-bonds with water implies an unexpected transient hydrophilic environment inside the nanotube and suggests a slow diffusion of water molecules along the channel. To check this hypothesis we analyzed our trajectories to determine the self-diffusion coefficient difference between the solvent molecules inside and outside the SPN, an observable that provides useful information on the corresponding diffusional behavior (see Materials and Methods). The self-diffusion coefficient of the water molecules in the nanotube interior is very low, varying between 0.13×10^{-5} and 0.0025×10^{-5} cm^2 s^{-1}, compared to the pure solvent (3.5×10^{-5} cm^2 s^{-1}).[27] The monodimensional self-diffusion

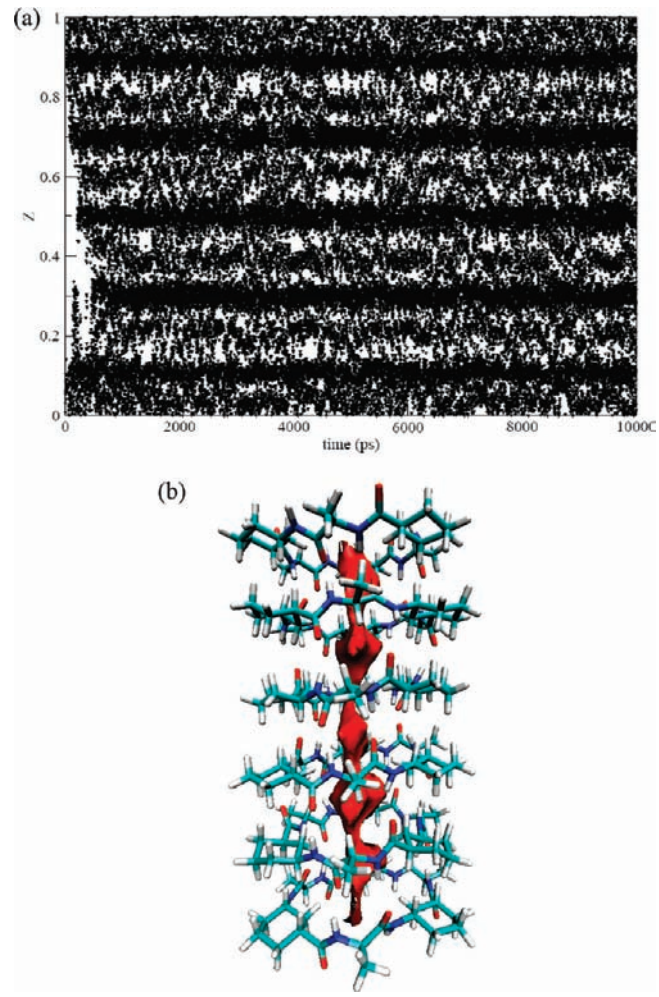

Figure 7. (a) Time evolution of the position of all the water molecules visiting the nanotube during the 20 ns of MD simulation. Note the higher density of the water in those regions located between the planes of the cyclic peptides and the sporadic empty regions at several locations and different times. (b) Interaction energy surface between a carbon probe and the SPN as obtained by CMIP calculations.

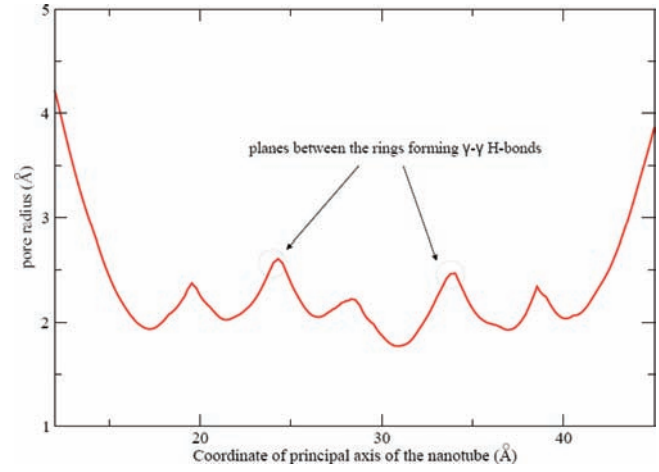

Figure 8. Effective pore radius of the nanotube calculated with HOLE. Larger values can be observed for the regions between ring planes.

coefficient computed in selected cases was approximately three times larger than the value cited above, confirming that the diffusion is mainly due to the water movement along the

(26) Smart, O. S.; Goodfellow, J. M.; Wallace, B. A. *Biophys. J.* **1993**, *65*, 2455.
(27) Water self-diffusion coefficient was calculated by using the 10 water molecules spending more time in the interior of the SPN.

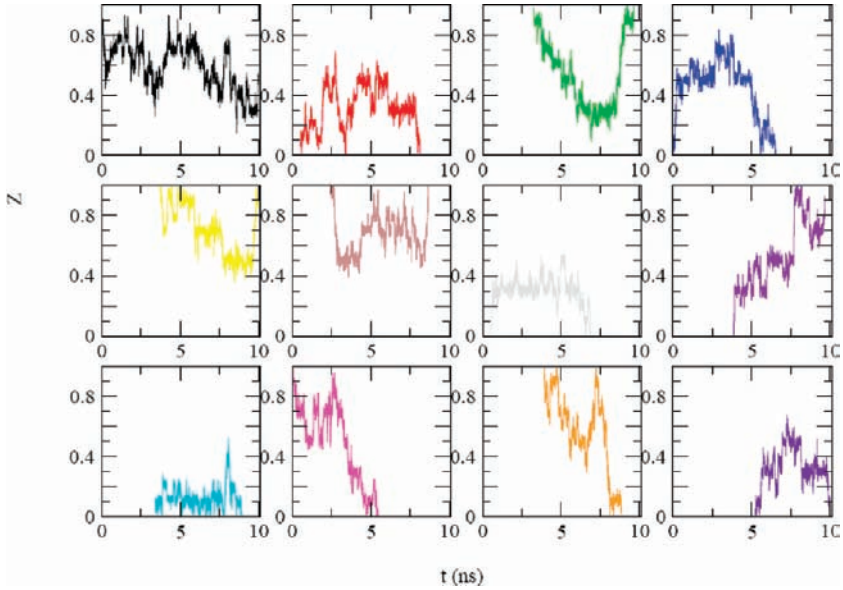

Figure 9. Schematic representation of the position of selected water molecules inside the peptide nanotube. Z represents the normalized coordinate of the nanotube principal axis.

SPN major axis (see eq 3 in Materials and Methods). Certainly, as anticipated, the ability of the interior of the SPN to form H-bonds with the aqueous solvent leads to a slow self-diffusion of water inside the channel and justifies the small number of water molecules which are able to explore the entire channel in the simulation time (Figure 9). In the case of chloroform, the diffusion of solvent molecules inside the nanotube is ~8 times slower than that observed for the free chloroform molecules,[28] a result that can be explained considering the steric restrictions inside the channel, the hybdrophobicity of the interior of the cavity (in the absence of solvent with H-bond donor/acceptor properties), and the hydrophilic nature of the nanotube ends due to the presence of unsatisfied H-bond groups.

MD simulations reveal then the complexity of the transport scenario of SPNs. The partially hydrophobic internal cavity is permeable to polar molecules but only of reduced size; in fact, using bigger but polar molecules, i.e. methanol, the passage is inhibited. Dynamics rather than structure is responsible for the water-coordinating ability of the nanotubes. Thus, short-range internal dynamics leads to the reversible formation/loss of H-bonding interactions of the peptide with small polar molecules in the interior of the channel. These transient hydrogen bonds, and the possibility to define strings of waters, explain why the SPN can coordinate water molecules with only a 4 kJ mol^{-1} cost, when the dehydration free energy of one water molecule is four times larger. However, intermolecular SPN−water H-bonds slow down the transport of water and the same is likely to happen with other small polar solvents able to fit inside the cavity. The situation with apolar molecules is clearly different; in fact, in the absence of polar solvents disturbing the intramolecular CP−CP interactions, the cavity interior is quite hydrophobic and seems to behave as a good container for small apolar molecules, since the hydrophilicity of the ends hinders the exit of the apolar molecules to the exterior. It remains to be investigated whether or not such properties makes α,γ-SPNs good containers for molecular hydrogen or other small and difficult to store molecules.

4. Conclusions

This is, to our knowledge, the first complete theoretical study of the structure, dynamics, deformability, energetics, and transport properties of a promising class of self-assembling nanotubes, composed of alternating D-α-amino acids and (1*S*,3*S*)-3-aminocyclohexanecarboxylic acids, in water, methanol, and chloroform, by means of molecular dynamics simulations. The SPN appears as a very stable structure, especially in nonpolar solvents, mostly due to formation of a complete network of intercyclopeptide hydrogen bonds, where α,α H-bonds appear to be more stable than the γ,γ ones, especially in water. The nanotube is globally very rigid (even more than DNA and similar to the interior of proteins) but, at the same time, displays remarkable solvent-dependent local flexibility. Such flexibility allows the generation of H-bonds with the solvent and, hence, the creation of a partial hydrophilic interior in the SPN, which explains the surprisingly good ability of the interior of the nanotube to coordinate water and also the quite slow kinetics of its transfer process. These transport properties combined with the high stability of the channel in different solvents (including very apolar ones) suggest that these nanotubes can act as good channels for transporting small polar molecules across biological membranes. On the contrary, in the presence of apolar molecules the interior remains fully hydrophobic and becomes an excellent container for apolar solvents like chloroform, which displays a low k_{on}, to enter into the channel but, once inside, resides inside for long periods of time. Future investigations will explore the transport properties of nonpolar molecules of different sizes, as well as the effect of the ring size and the axial length on the SPN thermodynamics. Overall, the present results demonstrate the power

(28) Lamoureux, G.; Faraldo-Gomez, J. D.; Krupin, S.; Yu. Noskov, S. *Chem. Phys. Lett.* **2009**, *468*, 270.

of theoretical calculations when acting as an atomic microscope to analyze the fine details of a complex supramolecular structure.

Acknowledgment. M.D. and R.G.F. are postdoctoral fellows of the Spanish Ministry of Science and Innovation. This work was supported by the Spanish Ministry of Education and Science (BIO2006-01602 and GEN2003-20642-CO9-07), Fundación Marcelino Botín, and Consolider Project on Supercomputation. All calculations were carried out on the *MareNostrum* supercomputer at the Barcelona Supercomputer Center and on local computers at the Institut de Recerca Biomèdica. J.R.G. also thanks the Spanish Ministry of Education and Science and the ERDF [(SAF2007-61015) and Consolider Ingenio 2010 (CSD2007-00006)] for financial support.

Supporting Information Available: Supporting figures, tables, and methods that complement the article are available. This material is available free of charge via the Internet at http://pubs.acs.org.

JA903400N